ENTE PER LE NUOVE TECNOLOGIE,
L'ENERGIA E L'AMBIENTE

Dipartimento Innovazione

A REFLECTIVITY PROFILOMETER FOR THE OPTICAL CHARACTERISATION OF GRADED REFLECTIVITY MIRRORS IN THE 250 nm - 1100 nm SPECTRAL REGION

ALESSANDRO COLUCCI, ENRICO NICHELATTI

ENEA - Dipartimento Innovazione
Centro Ricerche Casaccia, Roma

RT/INN/98/5

Testo pervenuto nel aprile 1998

ABSTRACT

We have developed the prototype of an instrument that can be used for the optical characterisation of graded reflectivity mirrors at any wavelength in the spectral region from 250 nm to 1100 nm. The instrument utilises a high-pressure Xe arc lamp as light source. Light is spectrally filtered by means of a grating monochromator. The sample is illuminated with an image of the monochromator exit slit. After reflection from the sample, this image is projected onto a 1024-elements charge-coupled device linear array driven by a digital frameboard and interfaced with a personal computer. We have tested the instrument accuracy by comparing measurement results with the corresponding ones obtained by means of a laser scanning technique. Measurement RMS repeatability has been estimated to be approximately of 0.8%.

[GRADED REFLECTIVITY MIRRORS, OPTICAL INSTRUMENTS, OPTICAL TESTING, PROFILING, REFLECTIVITY, THIN FILMS]

RIASSUNTO

È stato sviluppato il prototipo di uno strumento per la caratterizzazione ottica di specchi a riflettività variabile, operante a qualsiasi lunghezza d'onda nell'intervallo spettrale da 250 nm a 1100 nm. La sorgente dello strumento è una lampada ad arco allo Xenon ad alta pressione. La luce è filtrata spettralmente per mezzo di un monocromatore a reticolo. Il campione viene illuminato da un'immagine della fenditura d'uscita del monocromatore. Dopo esser stata riflessa dal campione, questa immagine viene proiettata su un array CCD lineare a 1024 elementi, connesso elettronicamente a una scheda digitale e interfacciato a un personal computer. L'accuratezza dello strumento è stata verificata confrontando alcune misure con le corrispondenti misure ottenute mediante una tecnica a scansione laser. La ripetibilità RMS delle misure è stata stimata essere circa dello 0.8%.

Contents

1 Introduction

It has been demonstrated, both theoretically and experimentally, that use of smooth radially graded reflectivity mirrors (GRM's) can significantly improve the performance of lasers equipped with unstable optical cavities [1-11].

When a GRM is utilised as the output coupler of an unstable laser cavity, the properties of the resonant modes and of the laser beam emerging from the cavity are strongly influenced by the reflectivity characteristics of the GRM. These characteristics can be essentially described in terms of the GRM reflectivity profile, where for *reflectivity profile* we mean the ratio of the intensity reflected from the GRM to the incident intensity, sampled along the GRM diameter.

In the literature one can find a number of papers dealing with the optical characterisation of GRM's [5,10-16]. In these papers the GRM reflectivity profile is measured essentially by scanning the GRM surface with a laser beam, which can be focused onto the sample [5, 10-15] or spatially filtered [16], and by measuring the reflected intensity. Even though an instrument based on this laser scanning technique generally provides accurate and reliable measurements [15], we believe that it has a major drawback in that the use of a laser source makes the instrument utilisable only at the laser wavelength or at a certain set of wavelengths within the laser emission spectral range; availability of wavelengths within a wide spectral region would be possible by using an optical parametric oscillator as laser source, but this would significantly increase the instrument cost.

In this paper we illustrate the characteristics of the prototype of an instrument, hereafter referred to as *reflectivity profilometer*, we have developed with the aim of measuring the reflectivity profile of GRM's at any wavelength in the spectral region from 250 nm to 1100 nm. This reflectivity profilometer is capable of measuring reflectivity profiles over a length of 7.21 mm along the sample diameter, with a spatial resolution of 7.04 μm. It utilises a Xe arc lamp as light source, which is spectrally filtered by a grating monochromator. Reflectivity profile measurements are essentially performed by illuminating the sample with an image of the monochromator exit slit, and by detecting the light reflected from the sample by means of a 1024-elements charge-coupled device (CCD) linear array. Note that because backface contributions to the sample reflection can perturbate the measurement results, the reflectivity profilometer is capable of characterising only GRM's which do not reflect from their backface, e.g. GRM's with an antireflection coated backface, or with wedge angled surfaces. As a completion of the instrument, a least-square-fit procedure for the elaboration of the measurement results is implemented for GRM's of the super-Gaussian type [10].

2 Description of the instrument

The optical layout of the reflectivity profilometer is schematically represented in Fig. 1. A 75 W high-pressure Xe arc lamp, L, which has essentially a continuous emission spectrum

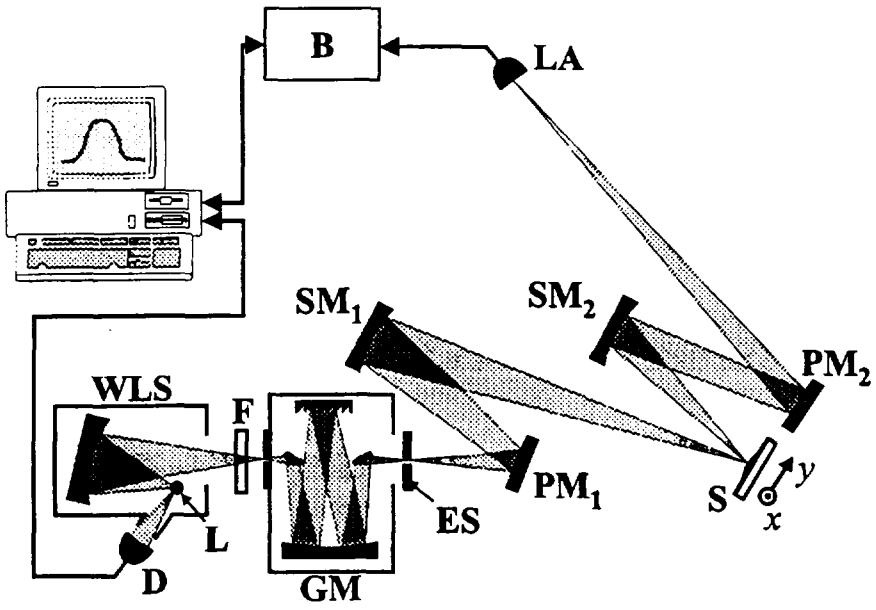

Figure 1 Schematic set-up of the reflectivity profilometer. PM_1 and PM_2 are fully reflecting plane mirrors. The largest sides of the exit slit ES, of its image on S, and of the CCD linear array LA lie along the x axis, which is perpendicular to the page plane.

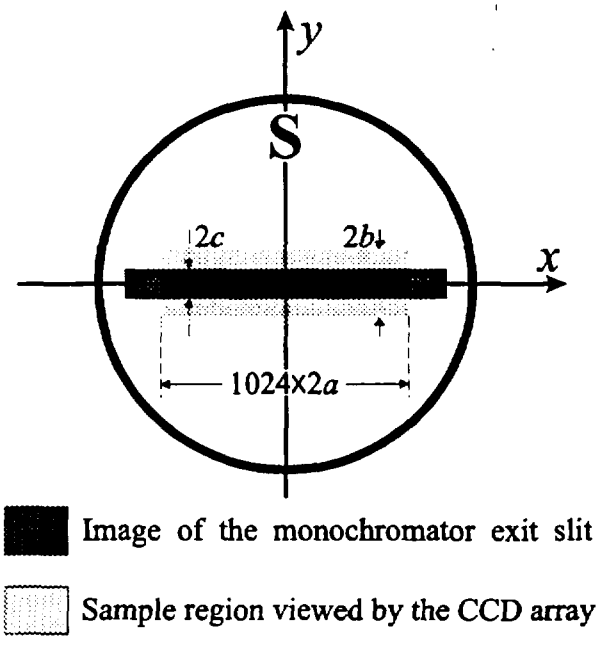

Figure 2 Front vision of the sample S. $2a$ and $2b$, height and width of the sample region viewed by each photodiode, respectively; $2c$, width of the monochromator exit slit image on the sample.

from 190 nm to 2.6 μm, is used as white light source, WLS. Lamp emission fluctuations are monitored by the silicon photodiode D, which provides a reference signal. The lamp housing is blower cooled and is equipped with a concave mirror which provides an effective *f*/3.4 beam focused at 76 mm in front of the housing. This beam is spectrally filtered by a 125 mm, *f*/3.7 grating monochromator, GM. A proper spectral bandpass filter, F, is inserted between WLS and GM to prevent wavelengths that could give rise to unwanted higher-order grating reflections from entering GM. A spherical mirror, SM_1, optically conjugates the GM exit slit to the sample plane, so that an 1:1 monochromatic image of this slit is formed on the sample S (see also Fig. 2). The size of this image is typically of about 0.4 mm×10 mm, but the image width (0.4 mm) can be adjusted at different values by properly setting the calibrated aperture of the GM exit slit. After reflection from S, the slit image is modulated in intensity by the reflectivity coefficient of the sample, which can vary along the illuminated area. This modulated image is then projected onto a linear array of detectors, LA, by means of the spherical mirror SM_2 which optically conjugates the sample plane to the array plane, with a magnification of about 3.55. LA is a 1024-elements CCD linear array driven by a 12-bit digital frameboard, B, and interfaced with a PC. The array can detect radiation in the spectral range from 250 nm to 1100 nm. The board clock frequency, which is of the order of 10 KHz, can be adjusted to obtain suitable signal-to-noise ratios under typical measurement conditions. The total size of the LA sensible area is 2.5 mm×25.6 mm; the size of each element is 2.5 mm×25 μm, and the element spacing is 25 μm centre-to-centre. Therefore, taking into account the magnification of the optical arrangement, the array can detect an effective sample area of approximately 0.704 mm×7.21 mm, with a spatial resolution of about 7.04 μm along its largest side, which lies along the x axis in Figs. 1 and 2. The sample is mounted on a micrometric x-y translation stage, so that it can be centred with respect to the slit image. To make this operation more accurate, the signal profile detected by LA can be displayed in real time on the PC video.

2.1 GRM characterisation procedure

The procedure for characterising a GRM essentially consists in measuring its reflectivity profile, and then fitting this profile with a suitable function. Most interest is focused at the moment on GRM's of the super-Gaussian type, which have been demonstrated to provide in a laser the optimum trade-off between a full exploitation of the active medium and high quality of the output beam [10,11]. Consequently, we have implemented a least-square procedure for fitting the measured reflectivity profiles with a super-Gaussian function plus a constant plateau, i.e.:

$$R_{GRM}(r) = (R_{MAX} - R_0) \exp[-2 (r / w)^N] + R_0 , \qquad (1)$$

where r is the radial distance from the GRM centre of symmetry, R_{MAX} and R_0 are the reflectivity maximum and minimum value, respectively; w is the GRM spot-size radius, and N is the index of super-Gaussianity. The value of R_0 accounts for residual reflectivity of the GRM antireflection coating.

Measurement of GRM reflectivity profiles is accomplished according to the photometric technique [17]: two subsequent measurements are taken of the light intensity reflected from the GRM and from a reference mirror of uniform known reflectivity R_{REF}, respectively. Both measurements have to be performed in a darkened environment. The GRM has to be centred with respect to the GM exit slit image by finely displacing the sample mount along the y direction. This operation is accomplished by maximising the width of the signal profile which is displayed in real time on the PC video.

Let $S_{GRM}(i)$ and $S_{REF}(i)$ be the normalised signals detected by the i^{th} photodiode of the CCD array, corresponding to the GRM and reference mirror measurement, respectively. Both signals are normalised with respect to the signal provided by the probe detector D in order to correct for lamp emission fluctuations. Then, one can write:

$$S_{GRM}(i) = \gamma R_{GRM}(i) I(i) + S_B(i), \tag{2}$$

$$S_{REF}(i) = \gamma R_{REF} I(i) + S_B(i), \tag{3}$$

where γ is the gain of the array photodiodes, $R_{GRM}(i)$ is the reflectivity of the GRM point $x(i)$ that optically corresponds to the i^{th} photodiode, $I(i)$ is the intensity of the radiation which impinges onto the same GRM point, and $S_B(i)$ is a background signal that can be generated by the detector dark current and by residual environmental scattered light. This background signal can be estimated by measuring a non-reflecting sample (for example, a black opaque surface) under the same conditions that occur during the measurement of $S_{GRM}(i)$ and $S_{REF}(i)$.

As the value of R_{REF} is known, we can derive from Eqs. (2) and (3) the following formula for the evaluation of the GRM reflectivity profile:

$$R_{GRM}(i) = \frac{S_{GRM}(i) - S_B(i)}{S_{REF}(i) - S_B(i)} R_{REF}, \quad i = 1, 2, ..., 1024. \tag{4}$$

Repeating for a number of times (typically of the order of 100) the measurement of $S_{GRM}(i)$ and $S_{REF}(i)$, one can improve measurement statistics and estimate the random error associated with the signal given by each photodiode of the CCD array, and therefore also the error associated with $R_{GRM}(i)$. The total measurement takes typically 3-5 minutes, yielding a set of 1024 couples of data $\{x(i), R_{GRM}(i)\}$ which represent the position along the GRM diameter and the reflectivity therein, respectively. However, owing to the instrument finite resolution cell, this result is an approximate one, as it will be discussed in the next subsection.

2.2 Instrument spatial resolution

Above we have considered Eqs. (2-4) to model the measurement of GRM reflectivity profiles.

However, in introducing Eqs. (2) and (3) we have disregarded the fact that the array photodiode elements have a finite size, and therefore that each one of them collects the light intensity reflected from a finite portion of the sample. To account for this fact, one should replace Eqs. (2) and (3) with the following ones:

$$S_{GRM}(i) = \frac{\gamma}{4ab} \iint_{\sigma(i)} R_{GRM}(x,y)\, I(x,y)\, dx\, dy + S_B(i), \tag{2'}$$

$$S_{REF}(i) = \frac{\gamma}{4ab} R_{REF} \iint_{\sigma(i)} I(x,y)\, dx\, dy + S_B(i), \tag{3'}$$

where $I(x,y)$ and $R_{GRM}(x,y)$ represent the illumination intensity and the GRM reflectivity at the point (x,y) of the sample surface, respectively, and the integration domain

$$\sigma(i) = [\, x(i) - a\, ,\, x(i) + a\,] \times [\, -b\, ,\, b\,]$$

is the rectangular region on the sample surface which is viewed by the i^{th} photodiode. In our case, $2a$ = 7.04 μm and $2b$ = 704 μm.

The effective domain of integration for the integrals that appear in Eqs. (2') and (3') is determined by the sample region where $I(x,y) \neq 0$. Let $2c$ be the y-width of $I(x,y)$ (see Fig. 2). Then the effective domain of integration is

$$\sigma'(i) = [\, x(i) - a\, ,\, x(i) + a\,] \times [\, -b'\, ,\, b'\,],$$

where $b' = \min(b,c)$. Therefore $2a \times 2b'$ is the resolution cell of our instrument.

Here one should also consider that the illumination wavelength varies from $-c$ to c along the y direction as a consequence of the monochromator grating dispersion. However, we can neglect this fact by assuming that the spectral bandwidth of the radiation impinging onto the sample is narrow enough to assume as constant the spectral response of the sample within this bandwidth. In our set-up this spectral bandwidth is typically set at 2-10 nm, depending on the aperture of the monochromator exit slit and on the type of grating which is utilised.

Assuming that the illumination $I(x,y)$ can be considered as constant over any resolution cell, and considering that for the characterisation of typical GRM's one is seldomly interested in spatial details finer than $2a$ = 7.04 μm (except that at the edge of GRM's with relatively high values of N), Eqs. (2') and (3') can be approximated as:

$$S_{GRM}(i) \cong \frac{\gamma}{2b} I[x(i),0] \int_{-b'}^{b'} R_{GRM}[x(i),y]\, dy + S_B(i), \tag{2''}$$

$$S_{REF}(i) \cong \frac{\gamma b'}{b} R_{REF}\, I[x(i),0] + S_B(i). \tag{3''}$$

Substituting these equations into Eq. (4), one finds:

$$R_{GRM}(i) = \bar{R}_{GRM}(i) \cong \frac{1}{2b'} \int_{-b'}^{b'} R_{GRM}[x(i), y]\, dy . \qquad (5)$$

This result means that $R_{GRM}(i)$ is an average $\bar{R}_{GRM}(i)$ of the GRM reflectivity in the y-direction: spatial details along the y axis that are smaller than $2b'$ result smoothed. This smoothing effect can perturbate the characterisation of GRM's of the super-Gaussian type: the super-Gaussian parameters w and N can be underestimated, depending on the values of these parameters and on the value of b', if one does not take into account expression (5) but simply considers expressions (1) and (4) for the fitting procedure. However, a simple criterion can be derived, by approximately integrating expression (5), that indicates under which conditions the measured reflectivity profile is unaffected by perturbations. In this case, expression (4) can be used for the fitting procedure without introducing these underestimations. In fact, by substituting function (1) into the integral of Eq. (5) (with $r = [x^2(i) + y^2]^{1/2}$), and approximating function (1) with its Taylor expansion up to the first order in y^2, one finds that expression (5) becomes equal to the super-Gaussian function (1) (with $r = |x(i)|$) minus the following perturbative term:

$$\varepsilon(i) = (R_{MAX} - R_0)\frac{N}{3}\left(\frac{b'}{w}\right)^2 \left(\frac{|x(i)|}{w}\right)^{N-2} \exp\left[-2\left(\frac{|x(i)|}{w}\right)^N\right].$$

It can be verified that $\varepsilon(i)$ is negligible if the following condition is satisfied:

$$(b'/w)^2 << 3/N \quad (\text{for } N \geq 2). \qquad (6)$$

Therefore, if condition (6) is likely to fail for a given super-Gaussian GRM, the measured profile can be affected by perturbations. Consequently, in this case the more accurate expression (5) has to be utilised in the fitting procedure to avoid systematic errors that would be introduced by use of expression (4).

3 Test of the instrument

Measurements performed with the reflectivity profilometer have been tested for accuracy and repeatability. To this purpose, we have measured the reflectivity profile along the diameter of a number of GRM's. The results of these measurements, performed at a wavelength λ = 633 nm, have been compared with the reflectivity profiles of the same GRM's obtained by scanning their surfaces with a focused HeNe laser beam, and measuring the reflected intensity

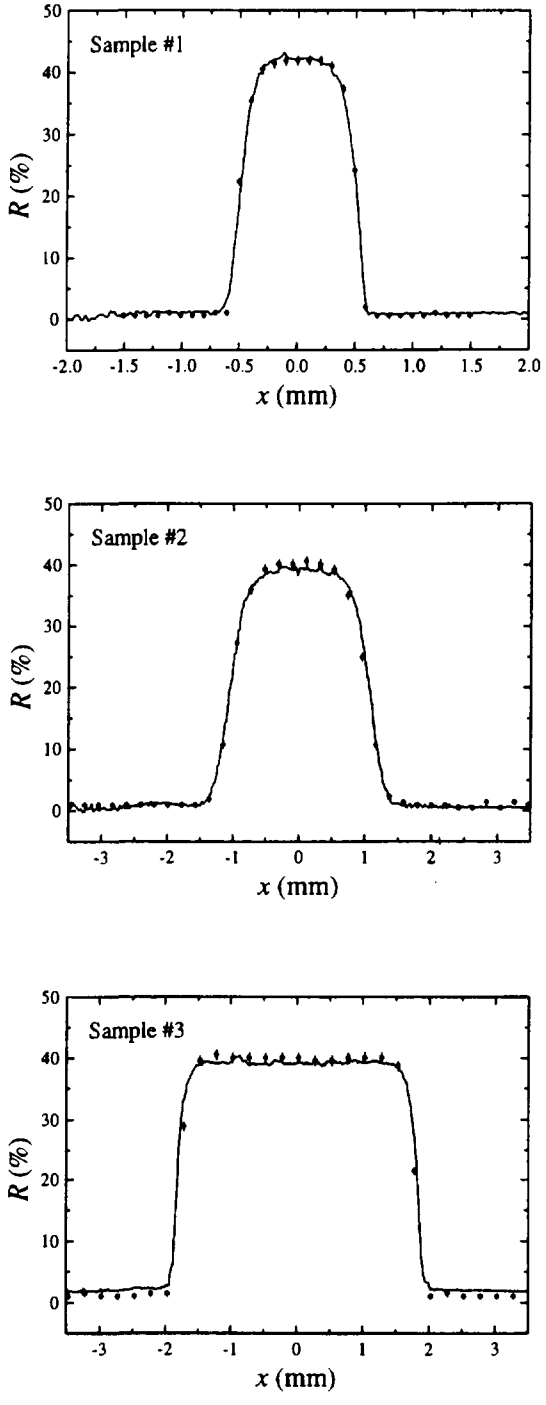

Figure 3 Reflectivity profiles of samples #1, #2, and #3 at λ = 633 nm, as measured with: the reflectivity profilometer (solid line); the HeNe laser scanning technique (dots).

by means of a photodiode and a lock-in amplifier. The diameter of the laser spot focused onto the sample was approximately of 60 μm, a value which is comparable to values previously reported in the literature [13,15]. The sample was scanned by moving the sample mount, which was fixed on a micrometric translation stage.

3.1 Measurement accuracy and repeatability

As an exemplificative set of the GRM's utilised to test the reflectivity profilometer, we consider here three thin-film GRM's, hereafter referred to as sample #1, #2, and #3, characterised by the following design:

substrate / 1.73H 0.687L H / air,

where H and L are quarterwave layers of TiO_2 (high index) and SiO_2 (low index), respectively. The optical thickness of the external TiO_2 layer is variable and is of a quarterwave at the centre of each GRM, and gradually goes to zero towards the substrate edge. We have utilised a BK7 substrate with a sand-blasted back-face, so that back-face contributions to reflectivity did not perturbate the optical characterisation. The depositions have been performed with an RF-sputtering apparatus and by means of the stationary mask technique (e.g., see Ref. 15). This technique essentially consists in shadowing the substrate, on which film growth takes place, with a mask having a circular hole of diameter D and positioned at a distance h from the substrate. We have used three different values of D to obtain different reflectivity profiles for the three samples, that is D=1 mm for sample #1, D=2.1 mm for sample #2, and D=3.5 mm for sample #3. For all the three samples we have chosen h = 0 mm with the aim of testing the reflectivity profilometer and the fitting procedure with the measurement of super-Gaussian GRM's characterised by a high value of N. (Indeed, as the mask is positioned very close to the substrate, its shadow is likely to present a sharp discontinuity in correspondence of the hole rim, this giving rise to the growth of a top-hat shaped film.) A high value of N can induce condition (6) to fail, considering that we expected to obtain values of w comparable with $D/2$ and that in our operating conditions we had $b' = c$ = 200 μm.

We have measured the reflectivity profiles of the three samples with both the reflectivity profilometer and the HeNe laser scanning technique. The bandpass of the monochromator was set at about 5 nm in our operating conditions. The results of these measurements are shown in Fig. 3. As one can notice, there is a quite good agreement between the profiles measured with the two systems.

To complete the characterisation of the three GRM's, we have used expression (1), with $r = |x|$, to fit the experimental profiles of Fig. 3, for both the reflectivity profilometer and the HeNe laser scanning technique measurement results. When fitting the profiles measured with the reflectivity profilometer, we have considered both expressions (4) and (5) in order to verify under which conditions use of expression (4) can give rise to systematic errors. The resulting best-fitting values of the parameters are listed in Tabs. 1 and 2. By comparing Tabs. 1 and 2, one can notice a good agreement between the values corresponding to the measurements performed with the HeNe laser scanning technique and the reflectivity profilometer. This indicates that the reflectivity profilometer provides measurements at least as accurate as those provided by the laser scanning technique. Moreover, one can notice in Tab. 2 that the values of w and N as estimated with expression (4) are slightly smaller than the corresponding ones estimated with expression (5), especially for samples #1 and #3. The reason for this is that condition (6) is poorly satisfied for samples #1 and #3, because sample #1 and#2 are

Sample #	R_{MAX} (%)	R_0 (%)	w (mm)	N
1	41 ± 2	0.5 ± 0.5	0.57 ± 0.02	9 ± 2
2	40 ± 2	0.9 ± 0.6	1.23 ± 0.04	5.6 ± 0.9
3	40 ± 1	1.0 ± 0.7	1.89 ± 0.03	19 ± 3

Table 1 Parameters of the fitting function (1) for the profiles measured with the HeNe laser scanning technique.

Sample #	R_{MAX} (%)	R_0 (%)	w (mm)	N
1	41 ± 1	0.75 ± 0.05	0.571 ± 0.005	8.1 ± 0.7
			(0.581 ± 0.005)	(8.6 ± 0.8)
2	39.4 ± 0.7	0.70 ± 0.05	1.25 ± 0.01	5.8 ± 0.3
			(1.26 ± 0.01)	(5.9 ± 0.3)
3	39.3 ± 0.7	1.5 ± 0.1	1.90 ± 0.01	21 ± 2
			(1.91 ± 0.01)	(26 ± 2)

Table 2 Parameters of the fitting function (1), as estimated by using expression (4), for the profiles measured with the reflectivity profilometer. The values between parenthesis are estimated by using expression (5), and they are reported only when they differ from the corresponding values estimated with expression (4).

characterised by a low value of w and a high value of N, respectively. Further, note that for samples #1 and #2 we have obtained relatively low values of N because the corresponding reflectivity profiles are smoother than the profiles expected from geometrical considerations on the mask shadow, even for the profiles measured with the HeNe laser scanning technique. To ascertain that these characteristics were real and did not depend on systematic errors introduced by the finite spatial resolution, we have measured the thickness profiles of the variable TiO_2 layers with a stylus profilometer having a nominal horizontal and vertical resolution of 2 μm and 1 Å, respectively. The measured thickness profiles were smooth and well agreed with the reflectivity profiles of Fig. 3. Taking into account also previously published experimental results [18], this smoothing effect can be attributed to scattering events taking place at the mask hole border and that can influence the shape of the growing film. However, a deepened study of the mask hole border influence on the film growth is beyond the aim of this work.

The RMS measurement repeatability of the reflectivity profilometer at the considered wavelength has been estimated by repeating for a number of times the measurement procedure for the above considered samples, and comparing the resulting reflectivity profiles. In this way we have found an RMS measurement repeatability of approximately 0.8%.

4 Conclusions

Realisation of a laser scanning system for the optical characterisation of devices having a variable reflectivity across their surface, such as GRM's, can represent a very expensive task when availability of wavelengths within a wide spectral region is required. We believe that the reflectivity profilometer here described can represent a suitable solution. Utilisation of a conventional arc lamp source, as compared to a set of laser sources or to an optical parametric oscillator, can keep the instrument cost reasonably low. Moreover, the relative simplicity of the set-up and the use of optical components which are available without difficulty in most optics laboratories should make this reflectivity profilometer attractive and easily realisable. We have tested the instrument at a wavelength of 633 nm, and it has been found to provide results which are in good agreement with those obtained by using a HeNe laser scanning system, with an RMS repeatability of approximately 0.8%.

We have discussed how the resolution cell size can influence estimation of the super-Gaussian parameters. We have also introduced a criterion, represented by condition (6), that permits to evaluate whether measured reflectivity profiles are affected by perturbations induced by the instrumental resolving power or not. However, it has been pointed out that use of expression (5) in the fitting procedure should provide accurate estimations of the super-Gaussian parameters even if the measured profile is affected by this kind of perturbations.

Acknowledgements

The authors thank A. Gentili for his skilful technical assistance, and G. Salvetti for valuable discussions.

References

[1] N. G. Vahitov, "Open resonators with mirrors having variable reflection coefficients," Radio Eng. Electron. Phys. **10**, 1439-1446 (1965).

[2] H. Zucker, "Optical resonators with variable reflectivity mirrors," Bell Syst. Tech. J. **49**, 2349-2376 (1970).

[3] A. Yariv and P. Yeh, "Confinement and stability in optical resonators employing mirrors with Gaussian reflectivity tapers," Opt. Commun. **13**, 370-374 (1975).

[4] G. Giuliani, Y. K. Park, and R. L. Byer, "Radial birefringent element and its application to laser resonator design," Opt. Lett. **5**, 491-493 (1980).

[5] P. Lavigne, N. McCarthy, and J. G. Demers, "Design and characterization of complementary Gaussian reflectivity mirrors," Appl. Opt. **24**, 2581-2586 (1985).

[6] E. Armandillo and G. Giuliani, "Achievement of large-sized TEM_{00} mode from an excimer laser by means of a novel apoditic filter," Opt. Lett. **10**, 445-447 (1985).

[7] N. McCarthy and P. Lavigne, "Large-size Gaussian mode in unstable resonators using Gaussian mirrors," Opt. Lett. **10**, 553-555 (1985).

[8] D. M. Walsh and L. V. Knight, "Transverse modes of a laser resonator with Gaussian mirrors," Appl. Opt. **25**, 2947-2954 (1986).

[9] A. E. Siegman, *Lasers* (University Science Books, Mill Valley, Calif., 1986), Chap. 23, pp. 913-922.

[10] S. De Silvestri, P. Laporta, V. Magni, O. Svelto, and B. Majocchi, "Unstable laser resonators with super-Gaussian mirrors," Opt. Lett. **13**, 201-203 (1988).

[11] S. De Silvestri, P. Laporta, V. Magni, and O. Svelto, "Solid-state laser unstable resonators with tapered reflectivity mirrors: the supergaussian approach," IEEE J. Quantum Electron. **24**, 1172-1177 (1988).

[12] C. Zizzo, C. Arnone, C. Calì, and S. Sciortino, "Fabrication and characterization of Gaussian mirrors for the visible and the near infrared," Opt. Lett. **13**, 342-344 (1988).

[13] G. Emiliani, A. Piegari, S. De Silvestri, P. Laporta, and V. Magni, "Optical coatings with variable reflectance for laser mirrors," Appl. Opt. **28**, 2832-2837 (1989).

[14] A. Piegari, A. Tirabassi, and G. Emiliani, "Thin films for special laser mirrors with radially variable reflectance: production techniques and laser testing," SPIE Proc. **1125**, 68-73 (1989).

[15] G. Duplain, P. G. Verly, J. A. Dobrowolski, A. Waldorf, and S. Bussière, "Graded-reflectance mirrors for beam quality control in laser resonators," Appl. Opt. **32**, 1145-1153 (1993).

[16] M. Montecchi, E. Nichelatti, A. Colucci, and E. Masetti, "Saw tooth phase modulating interferometry for the measurement of reflectivity and phase profiles of CO_2 laser mirrors," Pure Appl. Opt. **3**, 573-583 (1994).

[17] H. E. Bennet and J. M. Bennet, "Precision measurements of thin film optics," in *Physics of thin films*, G. Hass and R. E. Thun, eds. (Academic, New York, 1967), Vol. 4, pp. 57-69.

[18] E. Nichelatti, A. Tirabassi, and E. Melissano, "Deposition of profiled optical coatings by masking techniques: a study in the framework of the linear system theory," Pure Appl. Opt. **3**, 477-484 (1994).

Edito dall' ENEA
Unità Comunicazione e Informazione
Lungotevere Grande Ammiraglio Thaon di Revel, 76 - 00196 Roma
Stampa: Centro Stampa Tecnografico - C. R. Frascati

Finito di stampare nel mese di aprile 1998